

LOCAL THERMAL NON-EQUILIBRIUM FORCED CONVECTION OF A THIRD GRADE FLUID BETWEEN PARALLEL STRETCHING PERMEABLE PLATES EMBEDDED IN A POROUS MEDIUM

by

Mohammad Yaghoub ABDOLLAHZADEH JAMALABADI^{a*} and Majid OVEISI^b

^aDepartment of Mechanical, Robotics and Energy Engineering, Dongguk University,
Seoul, Republic of Korea

^bMaritime University of Chabahar, Chabahar, Iran

Original scientific paper
<https://doi.org/10.2298/TSCI160407198A>

The aim of this paper is the numerical investigation of local thermal non-equilibrium effects in the boundary-layer forced convection of a third grade fluid flowing in a porous medium confined by two parallel permeable stretching isothermal plates. The horizontal velocity of stretching walls is proportional to the longitudinal distance from origin while its vertical suction component is uniform. The porous medium obey the Brinkman extended Darcy momentum equation. The boundary-layer non-linear PDE are transformed by similarity solution to a system of ODE. The numerical investigation make known that a flow reversal come about the symmetry line of the channel attributable to the stretching plate boundary which diminished in highly Darcy numbers. The fluid-flow field and temperature distribution of the solid and fluid phases are studied based on the conductivity ratio, Darcy number, Prandtl number, Reynolds number, and third order fluid parameters.

Key words: *local thermal non-equilibrium, forced convection, stretching wall, third grade fluid, porous medium, temperature control*

Introduction

The flow of the third grade fluids model as in the biofluids applications such as blood [1] and the porous medium application [2] as the osseous tissues and organs such as arachnoid villi [3] has being on the center of attention of researchers in recent years [4]. In addition boundary-layer control by using suction of blowing and porous matrix has many applications in other engineering areas for instance in the design of filters, electronic cooling, particle separation, *etc.* As a result of non-linear requirement, the analysis of the flow behavior of non-Newtonian fluids exposes challenges to physicists, engineers and mathematicians. The equations that rule the non-Newtonian fluid-flow are of higher order, much more complex and restrained in contrast with Newtonian fluids. On the other hand there is not a solitary constitutive equation that can refer to the flow physical characteristics of all the non-Newtonian fluids. As a consequence of the multifaceted micro-structure of fluids, numerous models have been suggested to forecast the non-Newtonian performance. The third grade fluid is a differential type model proposed for a non-Newtonian fluid which has applications in pulp, petroleum, and polymer production industries and biochemistry [5, 6]. Misra [7] and Misra and Shit [8] proposed the numerical investigation of non-Newtonian viscoelastic fluid in a tissue channel with stretching walls with

* Corresponding author, e-mail: abdollahzadeh@dongguk.edu

applications to hemodynamics and biofluids. To find a heating protocol for hyperthermia its numerical and experimental is necessary. Hyperthermia simulation has need of a precise explanation of the velocity field which affects the thermal reaction of living materials [9-12].

It is remarked that the problem of local thermal non-equilibrium (LTNE) heat transfer of a non-Newtonian fluid (such as blood, oil, *etc.*) through a porous medium (such as oxygenators, kidney, lung, designed filters, *etc.*) with stretching boundary condition (such as extrusion of plastic sheets, filament from a die, *etc.*) which has application in dialysis of blood, textile coating, food processing, oil purification, heat storage beds in the environment and industry, has not been accomplished hitherto. The current investigation is an effort in this route that accepts the guaranteed of valuable applications in manufacturing stretching sheet processes, biomedical industrial and clinical disciplines. The impact of numerous factors, for instance Reynolds number, Darcy number, and Prandtl number has been inspected. The velocity and temperature distribution under several circumstances are exemplified in correlations and graphical forms. By using the figures, several important predictions have been imaginable such as maximum temperature increase and non-Newtonian flow control for the duration of bio processes, surgery, and manufacturing processes.

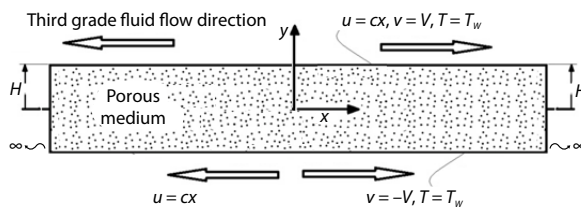


Figure 1. Schematic of system

In this study, the following assumptions are used: the fluid is an incompressible non-Newtonian fluid, thermophysical properties of the fluid are constant, buoyancy force is modeled with Boussinesq approximation, and the base fluid and the solid phases are not in thermal equilibrium. Then, the 2-D, $u(x, y)$ and $v(x, y)$, steady momentum conservation equations for this problem are expressed as:

Continuity:

$$\frac{\partial \rho u}{\partial x} + \frac{\partial \rho v}{\partial y} = 0 \quad (1)$$

x-momentum equation:

$$\begin{aligned} u \frac{\partial u}{\partial x} + v \frac{\partial u}{\partial y} = v \frac{\partial^2 u}{\partial y^2} + \frac{\alpha_1}{\rho} \left(u \frac{\partial^3 u}{\partial x \partial y^2} + \frac{\partial u}{\partial x} \frac{\partial^3 u}{\partial y^2} - 3 \frac{\partial u}{\partial y} \frac{\partial^2 u}{\partial x \partial y} + v \frac{\partial^3 u}{\partial y^3} \right) \\ - \frac{\alpha_2}{\rho} \left(2 \frac{\partial u}{\partial y} \frac{\partial^2 u}{\partial x \partial y} \right) + 6 \frac{\beta_2 + \beta_3}{\rho} \left(\frac{\partial u}{\partial y} \right)^2 \frac{\partial^2 u}{\partial y^2} + \frac{v}{K} u \end{aligned} \quad (2)$$

Fluid energy conservation equation:

$$\rho_f C_{p,f} \left[\frac{\partial}{\partial x} (u T_f) + \frac{\partial}{\partial y} (v T_f) \right] = \frac{\partial}{\partial x} \left(k_f \frac{\partial T_f}{\partial x} \right) + \frac{\partial}{\partial y} \left(k_f \frac{\partial T_f}{\partial y} \right) + h_{sf} (T_s - T_f) \quad (3)$$

Problem statement

The schematic of the 2-D (x -, y -Cartesian co-ordinates) problem is illustrated in fig. 1. As plotted a third grade fluid heated in a porous medium by viscous dissipation and cooled by permeable walls (x -axis is symmetry line). The gap between parallel plates are $2H$ and fluid injection or suction (with filtration velocity of V) at $y = \pm H$.

Solid energy conservation equation:

$$0 = \frac{\partial}{\partial x} \left(k_s \frac{\partial T_s}{\partial x} \right) + \frac{\partial}{\partial y} \left(k_s \frac{\partial T_s}{\partial y} \right) + h_{sf} (T_f - T_s) \quad (4)$$

with the boundary condition of symmetry on the channel centerline:

$$\left. \frac{\partial u}{\partial y} \right|_{y=0} = \left. \frac{\partial T}{\partial y} \right|_{y=0} = v|_{y=0} = 0 \quad (5)$$

and the boundary condition of isothermal stretching wall with suction/injection:

$$u|_{y=H} = cx, v|_{y=H} = V, T|_{y=H} = T_w \quad (6)$$

the following dimensionless variables will now be introduced:

$$\xi = \frac{x}{H}, \eta = \frac{y}{H}, u = cx f', v = -cHf, \theta = \frac{T}{T_w} \quad (7)$$

It may be distinguished that the continuity eq. (1) is routinely satisfied by variables chosen in eq. (5). In terms of the non-dimensional variables (5), the eq. (2) reads:

$$f''' + \text{Re} (ff'' - f'^2) - \frac{f'}{\text{Da}} + \varepsilon_1 (2f'' f' - f f''') - (3\varepsilon_1 + 2\varepsilon_2) f'^2 + 6\varphi f'^2 f''' = 0 \quad (8)$$

where the $\text{Da} = K/H_2$ is Darcy number, $\varepsilon_1 = c\alpha_1/\mu$, $\varepsilon_2 = c\alpha_2/\mu$, and $\varphi = c^2 \zeta^2 (\beta_2 + \beta_3) \mu^{-1}$ where $\varphi = 0.01$, $\varepsilon_1 = 0.001$, and $\varepsilon_2 = 0.1$ are the nominal values for blood.

Furthermore the similarity equation of fluid energy, eq. (3), reads:

$$\theta_f'' + \text{RePr} f \theta_f' = \sigma (\theta_f - \theta_s) \quad (9)$$

and equation of solid energy, eq. (4), reads:

$$\theta_s'' = \frac{\sigma}{k_r} (\theta_s - \theta_f) \quad (10)$$

where the $\text{Pr} = \nu/\alpha$, $\text{Re} = cH^2/\nu$, $\sigma = H^2 h_{sf}/k_f$, $k_r = k_s/k_f$. By the use of variable transformation (7), the boundary conditions (5) and (6) turn out to be:

$$f''(\eta) = f(\eta) = \theta'(\eta) = 0 \quad \eta = 0 \quad (11)$$

and

$$f'(\eta) = 1, f(\eta) = -A, \theta(\eta) = 1, \eta = 1 \quad (12)$$

where the inject/suction parameter is $A = V/cH$. One can also compute the local friction coefficient defined:

$$c_{fx} = \frac{2\tau_w}{\rho(cx)^2} = 2 \frac{(\tau_{xy})_{y=H}}{\rho(cx)^2} \quad (13)$$

where $\text{Re}_x = cxH/V$

Results

In this study, the LTNE forced convection of a third grade fluid between parallel stretching permeable walls filled with a porous medium was investigated. The system of coupled non-linear ordinary differential and its boundary conditions *i. e.* Equations (8)-(12) has been solved numerically by shooting method. The transformed boundary-value problem into the equivalent initial-value problem is solved by a trial-and-error approach with initial

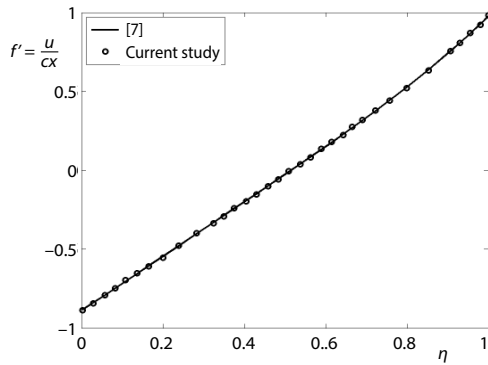


Figure 2. Axial velocity distribution for $Re = 1.0$, $Da = 1.0$, $\phi = \varepsilon_1 = \varepsilon_2 = 0.0$

study with that is done in fig. 2. As illustrated in fig. 2 the axial flow distribution of both solution are in a good agreement.

It is detected from fig. 3 that as Reynolds number increases, the y -component of velocity increase. In addition by increase of Reynolds number the u -component of velocity increase near the centerline while after about the 0.4 of maximum vertical distance up to the upper wall, it diminishes. By increase of Reynolds number heat absorption in the fluid increased, therefore, temperature of the system falls and both fluid and solid temperature profiles are flattened and tend to be reaching the wall temperature. In that cases the increase of the Reynolds number cause to increase the impact of wall on the fluid region by convective heat transfer mechanism. In case of temperature the Reynolds number has the same role as in velocity.

Figure 4 discloses that when Darcy number increases, initially the y -component of velocity increases near the symmetry line while after a certain height of the channel, beyond which it decreases. This remark approves with the concept, for the reason that the increase of Darcy number, decrease the solid matrix forces on the fluid. It is recognized that the solid force be pitted against the main streamline of the flow. Thus as the porosity of the porous media decrease, the flow of third grade fluid will be hampered. It is correspondingly renowned from the figure that the x -component of the velocity profile has three regions as: adjacent to the upper

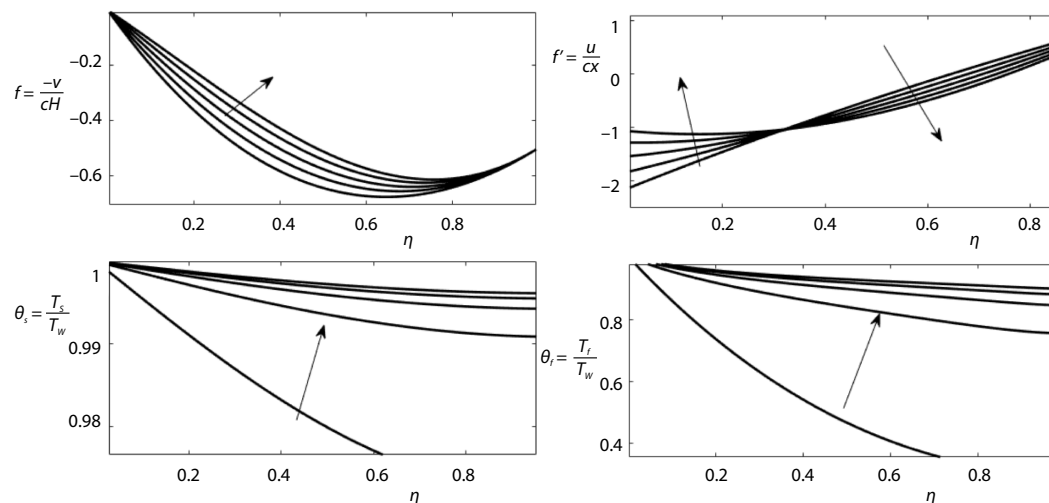


Figure 3. Effects of Reynolds number of 1, 2, 3, 4, and 5 on velocity and temperature field

guess of $f = -A\eta$, $\theta_f = \theta_s = 1$. The effects of various parameters are studied on the velocity components and temperature profiles in fluid and solid phases [13]. The figs. 3-11 the effects of Reynolds number from 0-5, Darcy number from 0.02 to 10^{-12} , ε_1 from 10^{-4} to 10, ε_2 from 0.1 to 1, ϕ from 0.01 to 0.1, A from 0.5 to 1, Prandtl number from 0.01 to 10, σ from 1 to 100, and conductivity ratio from 10 to 100 on velocity and temperature profiles while the fixed point is $Re = 5$, $Da = 10^{-12}$, $\varepsilon_1 = 10^{-4}$, $\varepsilon_2 = 0.1$, $\phi = 0.01$, $A = 0.5$, $Pr = 10$, $\sigma = 1$, and $k_r = 10$. As a benchmark problem the Misra [7] problem is considered and the comparison of the present

wall, bulk fluid, and the adjacent to the symmetry line. By increase of the Darcy number the x -component of velocity increase, decrease, and increase in the adjacent to the upper wall, bulk fluid, and the adjacent to the symmetry line regions, respectively. In all regions the increase of Darcy number cause the x -component of velocity profile to be more flattened. Indeed, increasing values of Darcy number show the large number of permeable spaces (the number of holes of the medium) which produce resistance to flow (fluid faces difficulties in inflowing through these holes) and decrease general fluid motion along with temperature distribution. This tendency to decrease the x -component of the velocity cause to weakened (as fluid has to devote exertion in moving through the porous medium) the effect of convective mechanism and so by increase of Darcy number both fluid and solid temperature profiles decrease and have a habit of increase of fluid temperature from the wall temperature over the all fluid domain. In that circumstances the increase of the velocity boundary thickness affect the influence of the thermal region.

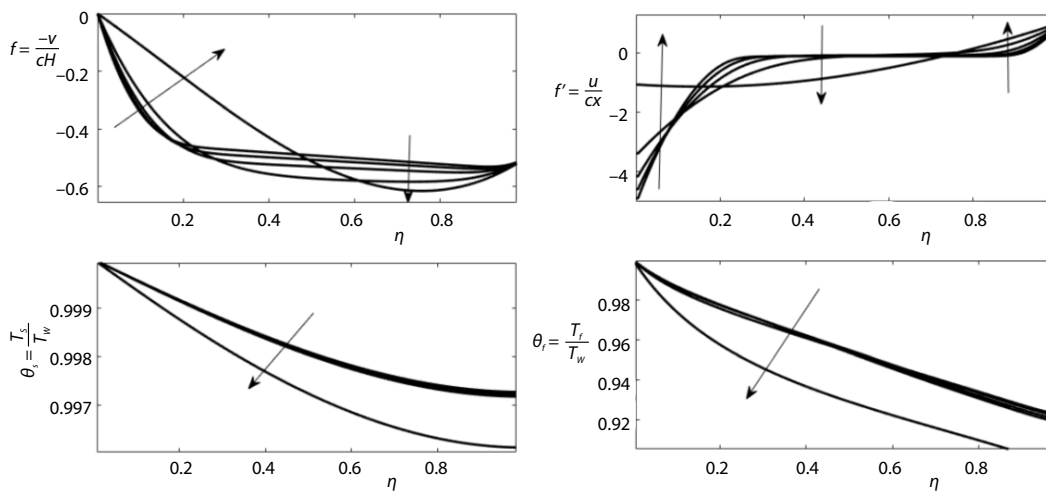


Figure 4. Effects of Darcy number of 10^{-12} , 0.05, 0.01, 0.015, and 0.02 on velocity and temperature field

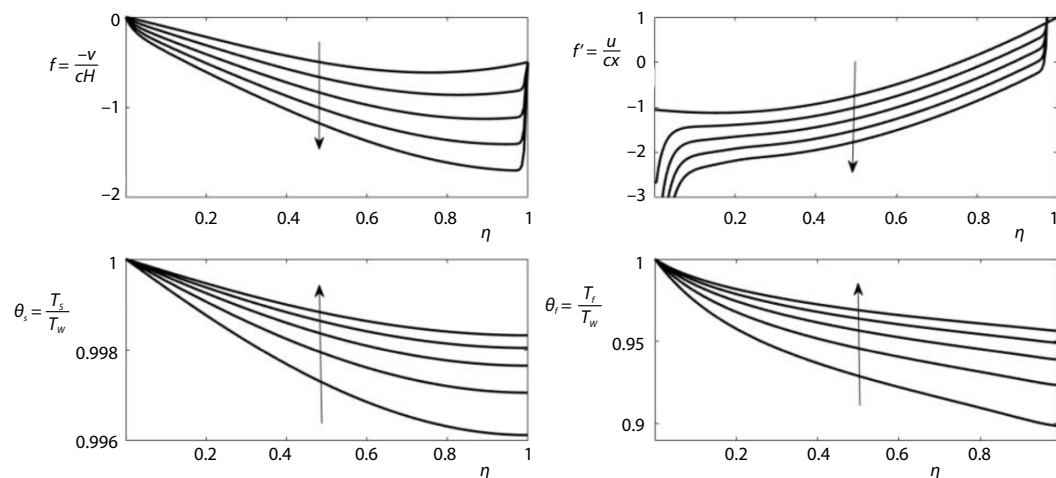


Figure 5. Effects of ϵ_1 of 10^{-4} , 2.5, 5, 7.5, and 10 on velocity and temperature field

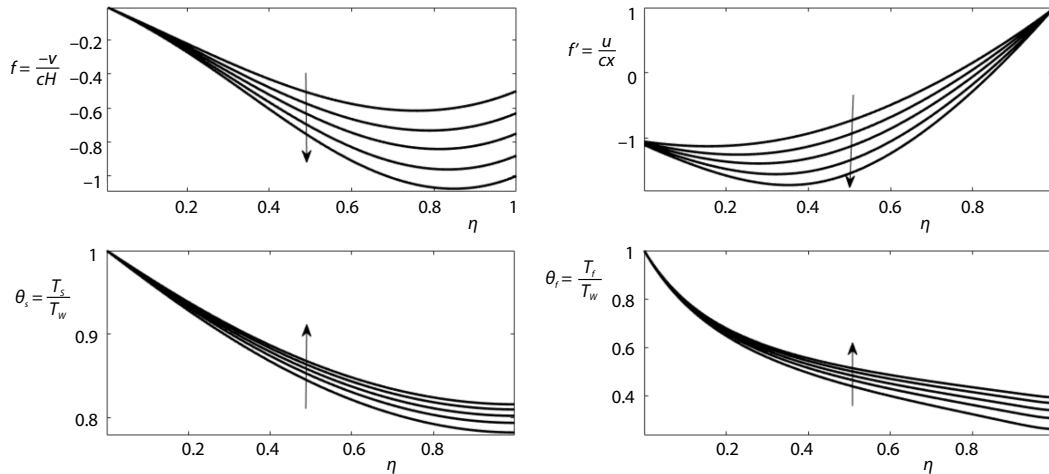


Figure 6. Effects of suction velocity of 0.5, 0.625, 0.75, 0.875, and 1 on velocity and temperature field

The effects of ε_1 and suction parameters on velocity components and temperatures are revealed in figs. 5 and 6. By increasing the second grade parameters ε_1 and ε_2 , the non-Newtonian effect increases as a result viscoelastic forces (inertia and elastic deformation) of the fluid come into play which compete against the fluid-flow. As presented the increase of ε_1 parameter cause the fluid motion towards the stretching sheets which decrease of velocity and gradient of velocity and increase of temperature end to end of the height of the channel. Due to elastic deformation outcome the boundary-layer thickness drops so the motion slows down. The same trend in retarding the fluid motion is seen for ε_2 in fig. 7 and φ in fig. 8 except the u -component of the velocity decrease near the symmetry line of the channel.

In the figs. 9-11 a fixed velocity profile is seen because the of Prandtl number, heat transfer parameter, and thermal conductivity ratio are the thermal parameters inherently. While the Prandtl number and conductivity ratio increase the temperatures monotonically all over the channel, the heat transfer parameter decrease it. As revealed in fig. 9, during the fluid motion the thermal boundary-layer thickness of the fluid decreases for increasing value

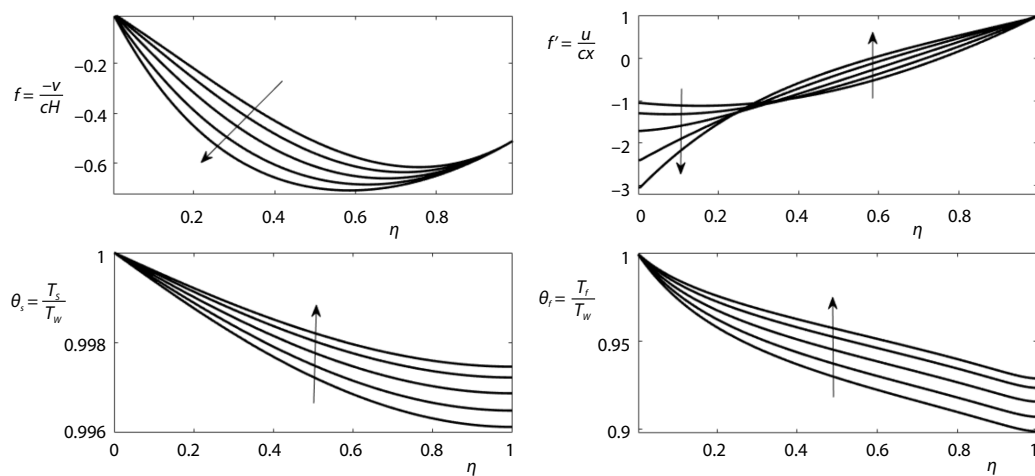


Figure 7. Effects of ε_2 of 10^{-1} , 0.1, 0.325, 0.55, 0.775, and 10 on velocity and temperature field

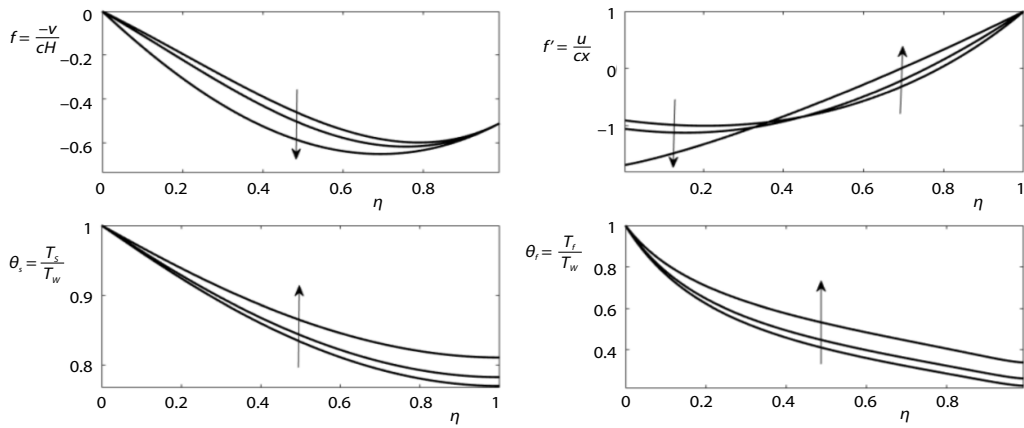


Figure 8. Effects of ϕ of 10^{-3} , 10^{-2} , and 10^{-1} on velocity and temperature field

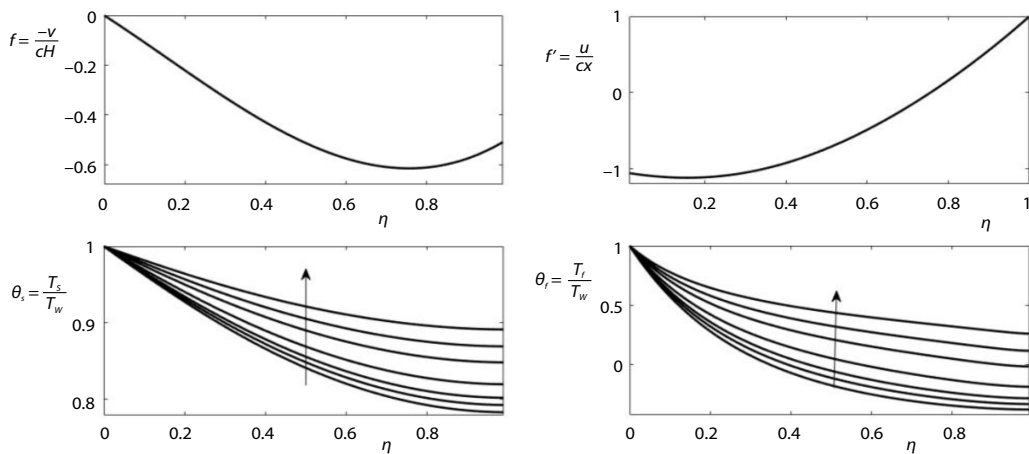


Figure 9. Effects of Prandtl number of 1, 1.5, 2, 3, 5, 7, and 10 on velocity and temperature field

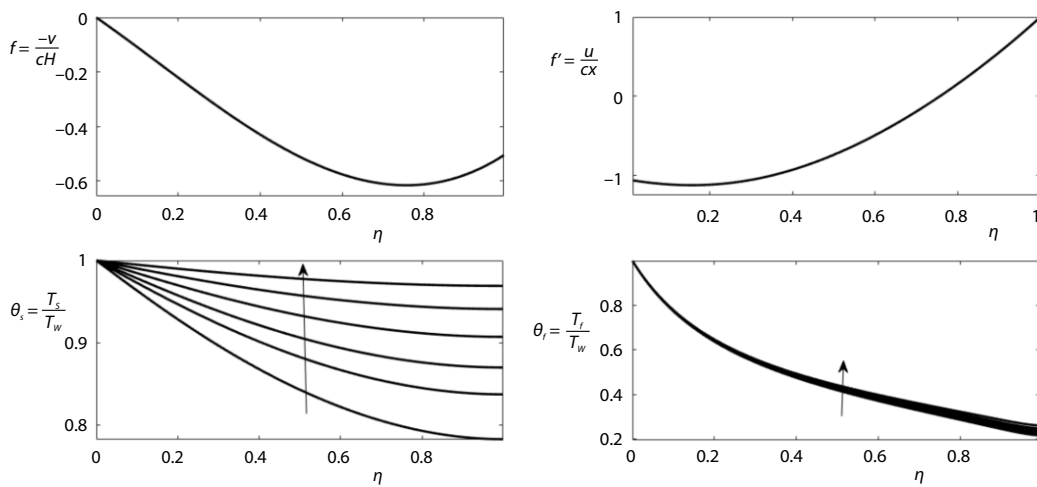


Figure 10. Effects of thermal conductivity ratio of 10, 15, 20, 30, 50, and 100 on velocity and temperature field

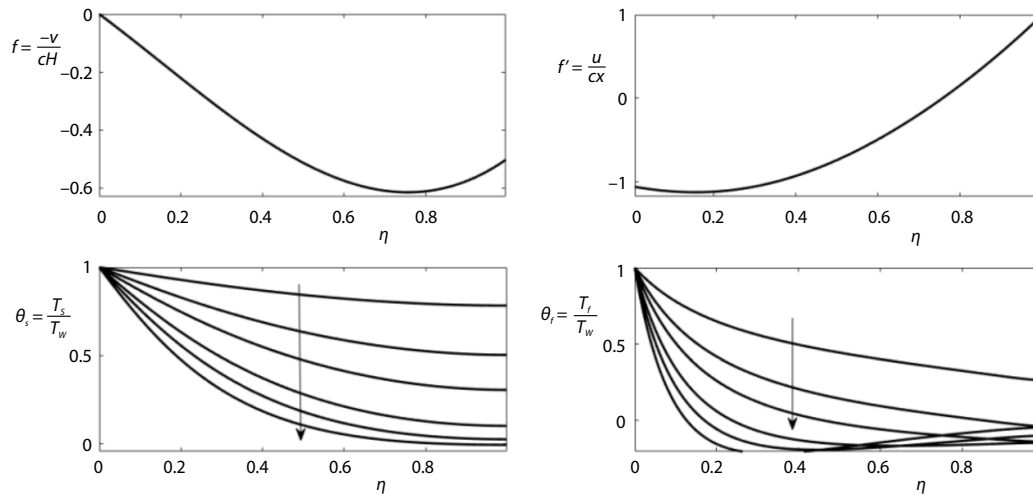


Figure 11. Effects of heat transfer parameter of 10, 20, 30, 50, 70, and 100 on velocity and temperature field

of Prandtl number. This can be attributed to the influence of conduction heat transfer due to thermal diffusivity in the flow. The influence is even more evident for small Prandtl number since the thermal boundary-layer depth is relatively large. Fluid temperature increases more than solid temperature at free spaces because the holes of the medium absorb more and more heat. The same phenomena cause the increase of the temperature by increase of thermal conductivity ratio. As disclosed in fig. 10, the effect of thermal conductivity ratio on fluid temperature profile is small as it not appeared directly in its governing equations. But by increase of solid thermal conductivity for a constant fluid, the solid can better follow the fluid temperature. Since the temperature difference between two phases and the heat exchange is decrease which causes the lower impact of fluid temperature. Henceforth effective cooling will be attained rapidly for the viscoelastic fluid with high thermal conductivity ratio. As demonstrated in fig. 11 the heat exchange parameter has the superior effect on the fluid and solid temperature in a non-equilibrium condition. It is distinguished that, on the contrary of Prandtl number effect, for any value of heat exchange parameter, temperature is

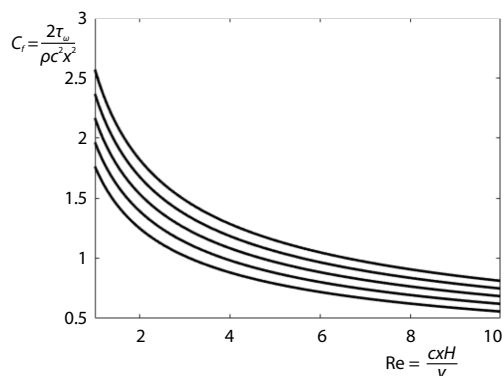


Figure 12. Skin friction coefficient vs. Reynolds number for various ε_1

not absolutely minimum at the upper wall and maximum near the centerline. By increase of heat exchange parameter the minimum of the fluid temperature can occurs in distance near the 0.3 of height of the channel from the centerline. Figure 12 demonstrates the effect of ε_1 on skin friction coefficient profile vs. the local Reynolds number in the upper wall. As Reynolds number increase, the skin friction coefficient decrease. By increase of third grade fluid parameter the value of skin friction coefficient is enhanced because of increase of non-linearity of the fluid, its higher viscous tension and film thickness near the wall.

Conclusions

In this study, we have thoroughly examined the effects of various parameters on the steady convective heat transfer in a porous channel. The main results can be summarized as follows.

- As Reynolds number increases, temperatures and velocity increases with the exception of the x -component of velocity decrease after 0.4 length ratio from symmetry line.
- As soon as Darcy number increases, temperatures decrease and the axial velocity profile is more flattened.
- The increase of ε_1 , A , φ , and ε_2 parameters cause the decrease of velocity and increase of temperature.
- Despite the fact that the Prandtl number and conductivity ratio increase the temperatures monotonically, the heat transfer parameter decreases it.
- By means of Reynolds number increase and ε_1 decrease, the skin friction coefficient decrease.

Nomenclature

A – suction parameter, [–]
 C_f – local friction coefficient, [–]
 C_p – heat capacitance, [$\text{Jkg}^{-1}\text{K}^{-1}$]
 c – velocity coefficient, [s^{-1}]
 Da – Darcy number, [–]
 H – half width of the channel, [m]
 h – heat transfer coefficient between phases, [$\text{Wm}^{-3}\text{K}^{-1}$]
 K – permeability of the medium, [–]
 k – thermal conductivity, [$\text{Wm}^{-1}\text{K}^{-1}$]
 Pr – Prandtl number, [–]
 Re – Reynolds number, [–]
 T – temperature, [K]
 (u, v) – velocity components, [ms^{-1}]
 V – filtration velocity at wall, [ms^{-1}]
 (x, y) – co-ordinates, [m]

Greek symbols

$\alpha_1, \alpha_2, \beta_2, \beta_3$ – the material constants in Cauchy stress tensor
 ν – kinematic viscosity, [m^2s^{-1}]
 ζ, η – non-dimension co-ordinates, [–]
 τ – shear stress, [Nm^{-2}]
 ρ – density of the fluid, [kgm^{-3}]

Subscripts

w – wall
 f – fluid
 s – solid

References

- [1] Abdollahzadeh Jamalabadi, M. Y. *et al.*, Influence of Radiative Heat Transfer and Transverse Magnetic Field on Peristaltic Flow of a Third Order Fluid in a Planar Channel, *Journal of Chemical and Pharmaceutical Research*, 7 (2015), 12, pp. 788-799
- [2] Abdollahzadeh Jamalabadi, M. Y., Effects of Micro and Macro Scale Viscous Dissipations with Heat Generation and Local Thermal Non-Equilibrium on Thermal Developing Forced Convection in Saturated Porous Media, *Journal of Porous Media*, 18 (2015), 9, pp. 843-860
- [3] Abdollahzadeh Jamalabadi, M. Y., Keikha, A. J., Fluid-Solid Interaction Modeling of Cerebrospinal Fluid Absorption in Arachnoid Villi, *Journal of Chemical and Pharmaceutical Research*, 8 (2016), 2, pp. 428-442
- [4] Ghasemi, S. E. *et al.*, Study on Blood Flow Containing Nanoparticles through Porous Arteries in Presence of Magnetic Field Using Analytical Methods, *Physica E*, 70 (2015), June, pp. 146-156
- [5] Moyers-Gonzalez, M. A. *et al.*, A Non-Homogeneous Constitutive Model for Human Blood – Part III: Oscillatory Flow, *Journal Non-Newton. Fluid Mech.*, 155 (2008), 3, pp. 161-173
- [6] Massoudi, M., Phuoc, T. X., Pulsatile Flow of Blood Using a Modified Second-Grade Fluid Model, *Comput. Math. Appl.*, 56 (2008), 1, pp. 199-211
- [7] Misra, J. C., Flow and Heat Transfer of a MHD Viscoelastic Fluid in a Channel with Stretching Walls: Some Applications to Haemodynamics, *Comp. Fluids*, 37 (2008), 1, pp. 1-11
- [8] Misra, J. C., Shit, G. C., Flow of a Biomagnetic Viscoelastic Fluid in a Channel with Stretching Walls, *ASME J. Appl. Mech.*, 76 (2009), 6, 061006

- [9] Craciunescu, O. I. , Clegg ,S. T., Pulsatile Blood Flow Effects on Temperature Distribution and Heat Transfer in Rigid Vessels, *Journal Biomech. Eng.*, 123 (2001), 5, pp. 500-505
- [10] Crane, L. J., Flow Past a Stretching Plate, *Z Angew Math. Phys.*, 21 (1970), 4, pp. 645-647
- [11] Ghani, F., *et al.*, Unsteady Magnetohydrodynamics Thin Film Flow of a Third Grade Fluid over an Oscillating Inclined Belt Embedded in a Porous Medium, *Thermal Science*, 21 (2017), 2, pp. 875-887
- [12] Hayat, T., *et al.*, Magnetohydrodynamic Flow of Nanofluid over Permeable Stretching Sheet with Convective Boundary Conditions, *Thermal Science*, 20 (2016), 6, pp. 1835-1845
- [13] Klamkin, M. S., Transformation of Boundary Value Problems into Initial Value Problems, *Journal Math. Anal. Appl.*, 32 (1970), 2, pp. 308-330